

# Cross sections at HERA\*

AHARON LEVY

The Raymond and Beverly Sackler School of Physics and Astronomy, Tel Aviv  
University, 69978 Tel Aviv, Israel

The energy dependence of cross sections is discussed as a way to learn about the dynamics of photon induced interactions at HERA. The question of determining the scale of exclusive electroproduction of vector mesons is addressed.

This talk is dedicated to the memory of Jan Kwiecinski.

## 1. Introduction

The energy dependence of a given process teaches us about the dynamics of this process. If the energy dependence can be described by a Regge-type approach a la Donnachie and Landshoff [1] we call the process soft. The total hadron-proton cross sections dependence on center-of-mass energy exemplifies the behaviour of soft processes.. If the energy dependence can be described by perturbative QCD (pQCD) we say that the process is hard. An example is exclusive  $J/\psi$  electroproduction [2, 3]. The nice feature of  $ep$  interactions at HERA is that we can see the interplay between soft and hard interactions [4].

Jan Kwiecinski made very many and important contributions to this subject by studying actually all possible reactions, like hadron-hadron ( $hh$ ),  $\gamma p$ ,  $\gamma\gamma$  and  $ep$ . Many of the studies that we have been doing at HERA were inspired by his findings. In this sense it is very appropriate that this conference is dedicated to his memory.

What sets the baseline for soft processes? Donnachie and Landshoff (DL) showed [1] that all  $hh$  total cross sections can be described by a simple expression containing two terms, inspired by Regge theory [5], one term

---

\* Talk presented at the 2009 Epiphany meeting, Cracow, Jan 5-7, 2009.

representing the contribution of the effective Pomeron trajectory and a second term of a Regge trajectory,

$$\sigma_{tot}(hh) = As^\epsilon + Bs^\eta \quad (1)$$

$$= As^{0.0808} + Bs^{-0.4525}, \quad (2)$$

where  $s$  is the square of the center-of-mass energy,  $A$  and  $B$  are process-dependent constants,  $\epsilon = \alpha_P(0) - 1$ ,  $\eta = \alpha_R(0) - 1$ , and  $\alpha_P(0)(\alpha_R(0))$  is the intercept of the effective Pomeron (Reggeon) trajectory. An example of  $s$  dependence of the total cross sections for  $\bar{p}p, pp, \pi^+p$  and  $\pi^-p$  interactions is shown in Fig. 1, together with the DL fits.

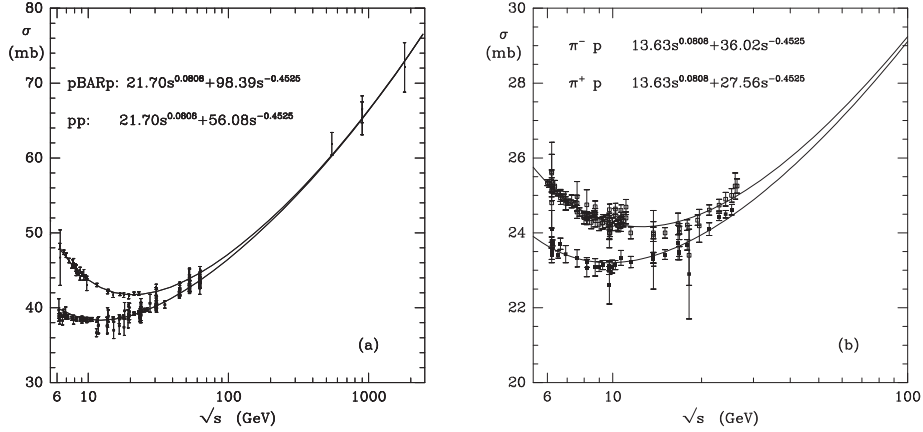


Fig. 1. The total cross section data of  $pp$ ,  $\bar{p}p$ ,  $\pi^+p$  and  $\pi^-p$  interactions. The curves are the DL fits to (2).

Thus, at high energies, the expected energy dependence for soft interactions is  $s^{0.08}$  or  $W^{0.16}$ , where  $W$  is the center-of-mass energy. A more recent fit to the total cross section data [6] results in a value  $\epsilon = 0.096$ .

When HERA started running there were quite extreme predictions for the value of the total photoproduction cross sections. They ranged from  $150 \mu\text{b}$ , compatible with the predictions of Donnachie and Landshoff, expected from a soft process, to values as high as  $1 \text{ mb}$ , coming from hard components which dominate the process. Seven seconds of running and a handful of events were enough to establish [7] that the photon behaves like a hadron at HERA energies, as seen in Fig. 2. The mild increase with energy indicated that the dominant configuration of the photon is its fluctuation in a large-size  $q\bar{q}$  pair.

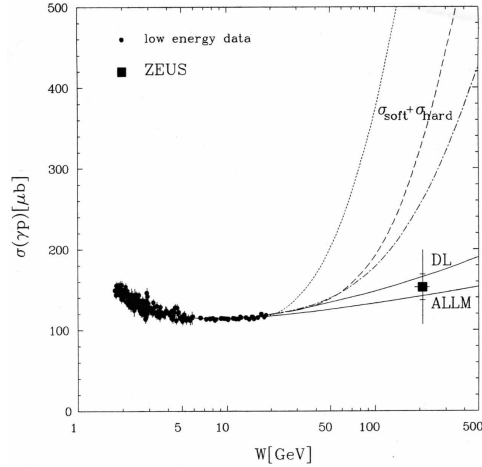


Fig. 2. The first total  $\gamma p$  cross section measured by ZEUS at HERA [7], together with low energy data. The curves are different predictions for the  $W$  behaviour of the cross section, before HERA started running.

## 2. Exclusive vector meson photoproduction

The total photoproduction cross section is plotted in Fig. 3, together with the cross sections for exclusive photoproduction of vector mesons,  $\sigma(\gamma p \rightarrow Vp)$ , as a function of  $W$ . One can describe the high energy part of the cross section by the form  $W^\delta$ , where for the total cross section  $\delta = 2\epsilon$ . The value of  $\delta$  for the light vector mesons  $\rho, \omega$  and  $\phi$  is also consistent with a soft process; here too the photon fluctuates into a pair of light  $q\bar{q}$  quarks and thus is in a large configuration. However, in case of the  $J/\psi$ , the pair of heavy quarks squeeze the photon into a small configuration, there is color screening and therefore the cross section is low. However, the pair being small, it can resolve the partonic structure of the proton. As the reaction is exclusive, the cross section is proportional to the gluon density squared. Since the gluon density rises strongly with decreasing Bjorken- $x$ , meaning increasing  $W$ , one gets a strong energy dependence in the case of the  $J/\psi$ . As the scale gets larger, where in this case the scale is set by the mass of the vector meson, the gluon density is steeper, resulting in a steeper  $W$  dependence. Thus the behaviour seen in Fig. 3 is a nice manifestation of the transition from soft to hard processes.

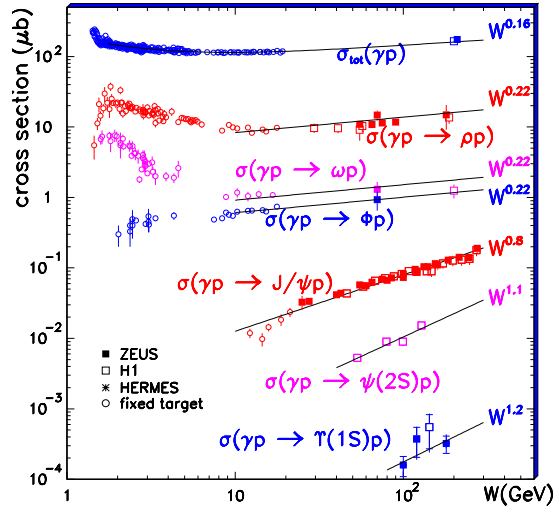


Fig. 3. Total and exclusive vector meson photoproduction data, as a function of  $W$ . The curves are fits of the form  $\sim W^\delta$ .

### 3. Exclusive vector meson electroproduction

In the earlier section, the scale was set by the vector meson mass. We can now fix the mass of the vector meson and use the virtuality  $Q^2$  of the photon as the scale. In this section we discuss the exclusive electroproduction of  $\rho^0$  [9, 10],  $\phi$  [11, 12] and  $J/\psi$  [2, 3]. In addition we also look at deeply virtual Compton scattering (DVCS) [13, 14], namely  $\gamma^*p \rightarrow \gamma p$ .

The cross section  $\sigma(\gamma^*p \rightarrow \rho^0 p)$  [9] is presented in Fig. 4 as a function of  $W$ , for different values of  $Q^2$ . The cross section rises with  $W$  at all  $Q^2$  values. In order to quantify this rise, the logarithmic derivative  $\delta$  of  $\sigma$  with respect to  $W$  is obtained by fitting the data to the expression  $\sigma \propto W^\delta$  for each  $Q^2$  value. The resulting values of  $\delta$  are shown in Fig. 4 and display a clear and significant rise from a value of  $\sim 0.1$ - $0.2$  at low  $Q^2$ , as expected for soft processes, to that of  $\sim 0.8$  at higher  $Q^2$ , which is consistent with twice the logarithmic derivative of the gluon density with respect to  $W$ .

An increase of the cross section  $\sigma(\gamma^*p \rightarrow \phi p)$  with  $W$  for different  $Q^2$  values is also observed, as displayed in Fig. 5. However, the data are not precise enough to see a change of the slope with  $Q^2$ .

The same situation is also true for  $\sigma(\gamma^*p \rightarrow J/\psi p)$  and for  $\sigma(\gamma^*p \rightarrow \gamma p)$ , shown in Fig. 6. For the latter, a recent measurement by the ZEUS collaboration, using the leading proton spectrometer, is shown in Fig. 7.

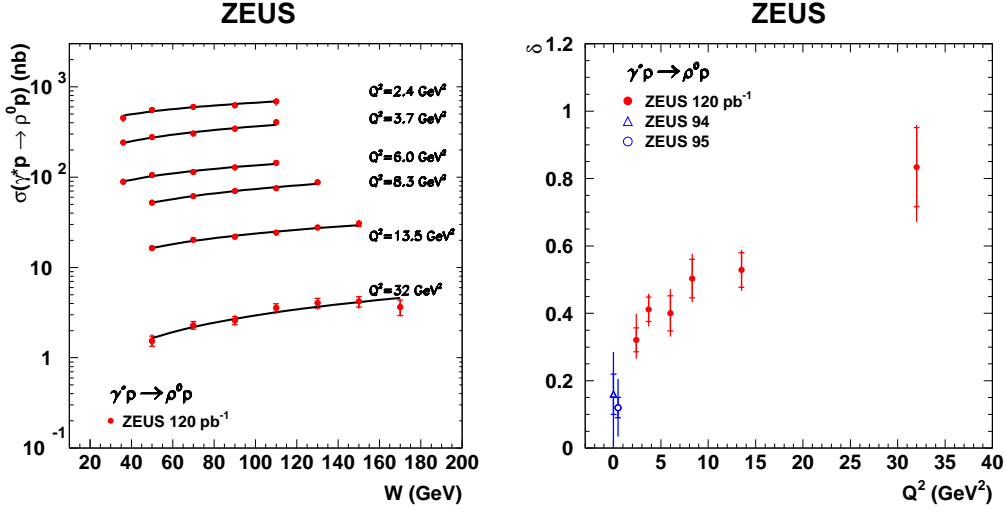


Fig. 4. (Left-hand side) The  $W$  dependence of the cross section for  $\gamma^* p \rightarrow \rho^0 p$  at different  $Q^2$  values. The curves are fits of the form  $\sim W^\delta$ . (Right-hand side) The  $Q^2$  dependence of  $\delta$ .

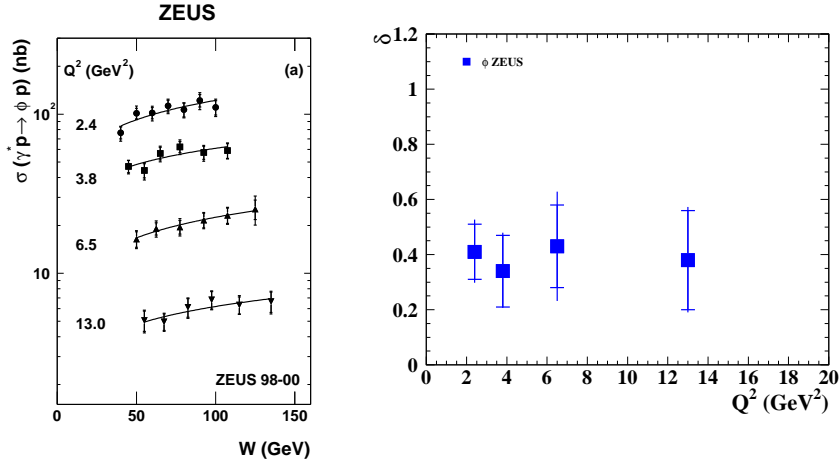


Fig. 5. (Left-hand side) The  $W$  dependence of the cross section for  $\gamma^* p \rightarrow \phi p$  at different  $Q^2$  values. The curves are fits of the form  $\sim W^\delta$ . (Right-hand side) The  $Q^2$  dependence of  $\delta$ .

Although the uncertainties on  $\delta$  are large also in this case, the trend of an increase with  $Q^2$  is apparent.

A compilation of all values of  $\delta$  for the different vector mesons,  $\rho^0$ ,  $\phi$ ,  $J/\psi$

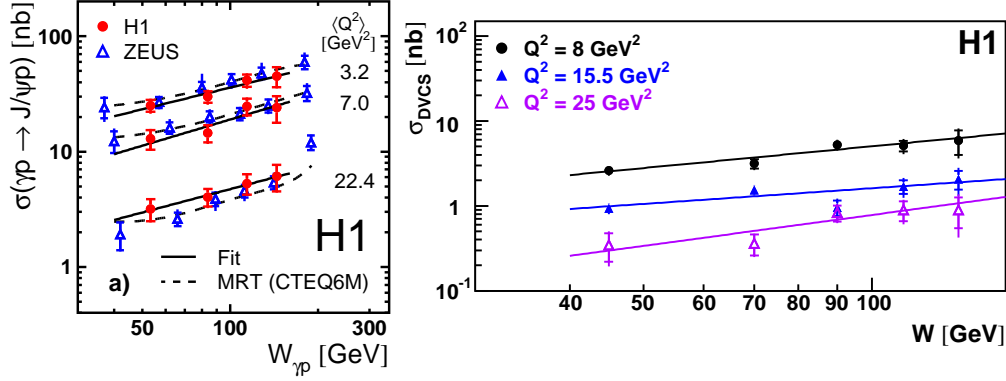


Fig. 6. (Left-hand side) The  $W$  dependence of the cross section for  $\gamma^*p \rightarrow J/\psi p$  at different  $Q^2$  values. The curves are fits of the form  $\sim W^\delta$ . (Right-hand side) The  $W$  dependence of the cross section for  $\gamma^*p \rightarrow \gamma p$  at different  $Q^2$  values, measured by the H1 collaboration. The curves are fits of the form  $\sim W^\delta$ .

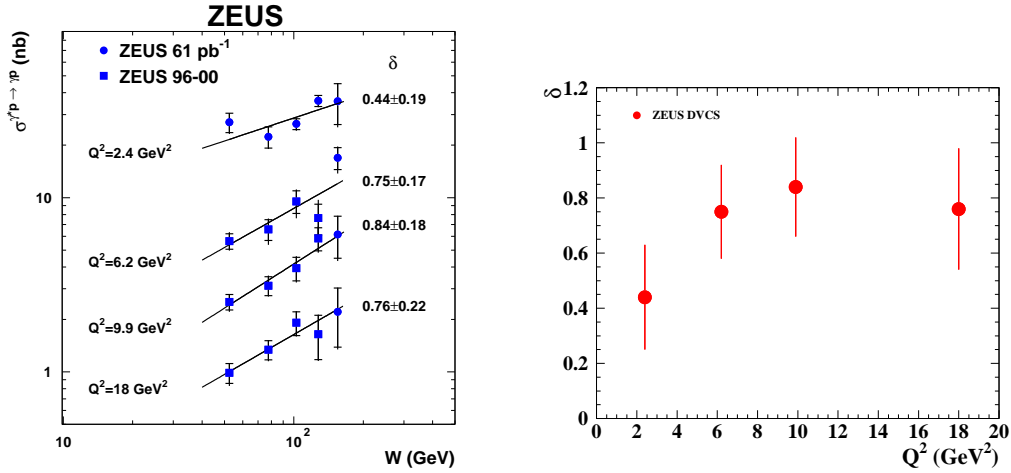


Fig. 7. (Left-hand side) The  $W$  dependence of the cross section for  $\gamma^*p \rightarrow \gamma p$  at different  $Q^2$  values, measured by the ZEUS collaboration. The curves are fits of the form  $\sim W^\delta$ . (Right-hand side) The  $Q^2$  dependence of  $\delta$ .

and DVCS, is shown in Fig. 8, as function of  $Q^2 + M^2$ , where  $M$  is the mass of the vector meson. One sees an approximate universal behaviour, showing an increase of  $\delta$  as the scale becomes larger, in agreement with the expectations mentioned above. The value of  $\delta$  at low scale is the one expected from the soft Pomeron intercept, while the one at large scale is in accordance with

that expected from the square of the gluon density. Note that the chosen scale of  $Q^2 + M^2$  might not be the appropriate effective scale for all the mesons. For further discussion about the effective scale, see section 4.3.

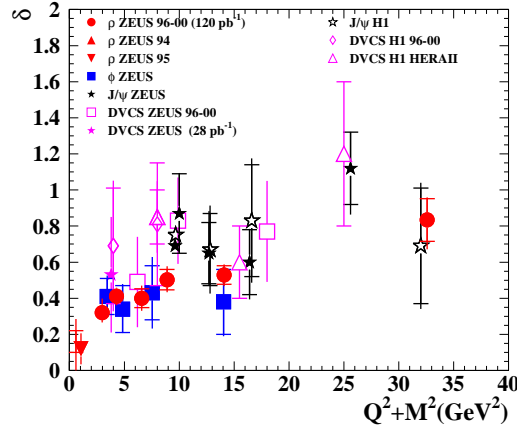


Fig. 8. A compilation of all values of  $\delta$  as a function of  $Q^2 + M^2$ , for exclusive electroproduction of  $\rho^0$ ,  $\phi$ ,  $J/\psi$  and DVCS.

#### 4. The ratio $\sigma(\gamma^*p \rightarrow Vp)/\sigma_{tot}(\gamma^*p)$

As we saw in the previous section, the cross section for exclusive electroproduction of vector mesons exhibits a rise with  $W$ , which becomes steeper with increasing  $Q^2$ . It is of interest to compare the  $W$  dependence of this cross section to that of the total  $\gamma^*p$  one. To this end we study the ratio

$$r_V \equiv \frac{\sigma(\gamma^*p \rightarrow Vp)}{\sigma_{tot}(\gamma^*p)}, \quad (3)$$

for different vector mesons, as a function of  $W$  for fixed  $Q^2$ . Before presenting the data, we discuss the expectations for  $r_V$  using pQCD and Regge arguments.

##### 4.1. expectations for $r_V$ in pQCD

In pQCD, the forward cross section for longitudinally polarized photons is expected [8] to behave as

$$\frac{d\sigma_L}{dt}|_{t=0} \propto \frac{1}{Q^6} \alpha_S(Q^2) [xg(x, Q^2)]^2, \quad (4)$$

where  $x$  is the Bjorken scaling variable,  $xg(x, Q^2)$  is the gluon density in the proton and  $t$  is the square of the four-momentum-transfer at the proton vertex.

Assuming an exponential  $t$  behaviour of the form  $d\sigma_V/dt \sim e^{bt}$ , one gets the following expectation:

$$r_V \propto \left(1 + \frac{1}{R}\right) \frac{W^{2\lambda}}{b} \approx \frac{W^{2\lambda}}{b}. \quad (5)$$

In expression (5) we have used the fact that both the gluon density distribution and the proton structure function have a similar  $x^{-\lambda(Q^2)}$  dependence and that the ratio  $R$  of the vector meson production cross section induced by longitudinal and transverse virtual photons,  $R = \sigma_L/\sigma_T$ , increases with  $Q^2$  but is  $W$  independent [9] and thus can be neglected.

#### 4.2. expectations for $r_V$ in the Regge approach

Using Regge phenomenology arguments [5], one expects  $\sigma_V \sim W^{4(\alpha_P(0)-1)}/b$  and  $\sigma_{tot} \sim W^{2(\alpha_P(0)-1)}$ , where  $\alpha_P(0)$  is the intercept of the Pomeron trajectory, and therefore

$$r_V \propto \frac{W^{2(\alpha_P(0)-1)}}{b}, \quad (6)$$

which is the same as (5), if we write  $\lambda = \alpha_P(0) - 1$ .

Both in pQCD and Regge approaches the ratio  $r_V$  rises with  $W$ . The  $W$  dependence is not strongly affected by  $b$  since both for the exclusive electroproduction of  $\rho^0$  and  $J/\psi$  shrinkage was found to be small [9, 2].

#### 4.3. Ratio - at what scale?

When calculating the ratio  $r_V$  one has to ensure that both cross sections are taken at the same hard scale, which we denote as  $Q_{eff}^2$ . Clearly, for the total inclusive cross section, the effective scale is  $Q^2$ . In Fig. 9 one can see the  $Q^2$  dependence of  $\lambda$  resulting from fitting the  $F_2$  data in the low- $x$  region ( $x < 0.01$ ) to the form  $F_2 \sim x^{-\lambda}$ . For photoproduction and the low  $Q^2$  region, the value of  $\lambda$  is in good agreement with that expected from the Pomeron intercept ( $\lambda = \alpha_P(0) - 1$ ). Starting at about  $Q^2 > 1 \text{ GeV}^2$ , the value of  $\lambda$  rises logarithmically with  $Q^2$ . It is of interest to see if  $r_V$  shows the expected  $W^{2\lambda}$  behaviour.

It is not clear what is the effective scale for exclusive vector meson electroproduction. One suggested scale, originally for the  $J/\psi$  [15], is

$$Q_{eff}^2 = \frac{Q^2 + M^2}{4}. \quad (7)$$



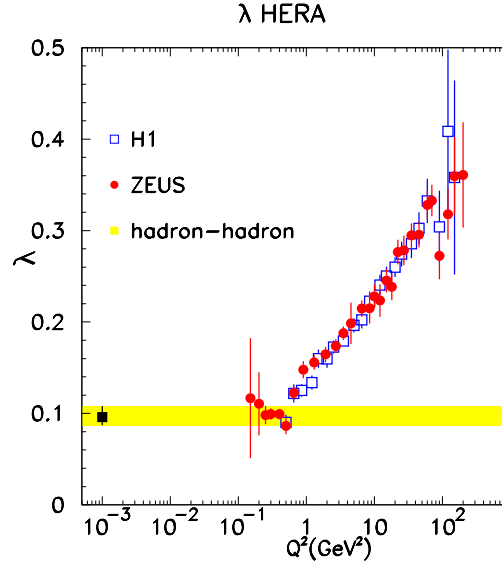


Fig. 9. The values of  $\lambda$ , obtained by fitting the proton structure function  $F_2$  to the form  $\sim x^{-\lambda}$ , as a function of  $Q^2$ . The shaded band shows  $\alpha_P(0)-1$  as obtained from hadron-hadron total cross section data.

where  $M$  is the mass of the vector meson. Frankfurt, Koepf and Strikman [16] calculated the effective scale for  $\rho$ ,  $J/\psi$  and  $\Upsilon$ , shown in Fig. 10, and find that their effective scale for the  $J/\psi$  and for the  $\Upsilon$  are significantly larger than that suggested by (7). One can parameterise [17] their effective

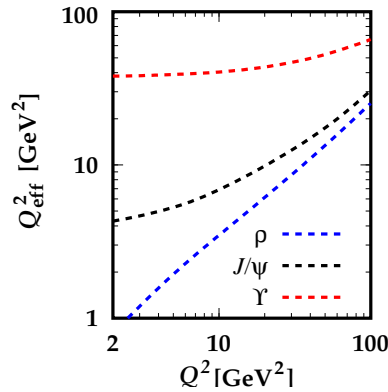


Fig. 10. The effective scale  $Q_{eff}^2$  as a function of  $Q^2$  for  $\rho$ ,  $J/\psi$  and  $\Upsilon$ .

scale for the  $\rho^0$  as

$$Q_{eff}^2 = \left( \frac{Q^2}{2.65} \right)^{0.887}. \quad (8)$$

As the most precise data at present are those of the exclusive electro-production of  $\rho^0$  [9], we will use these data to investigate the question of the effective scale. The ratio  $\sigma(\gamma^*p \rightarrow \rho^0 p)/\sigma_{tot}(\gamma^*p)$  is plotted in Fig. 11 as a function of  $W$ , for different fixed effective scales. Three effective scales

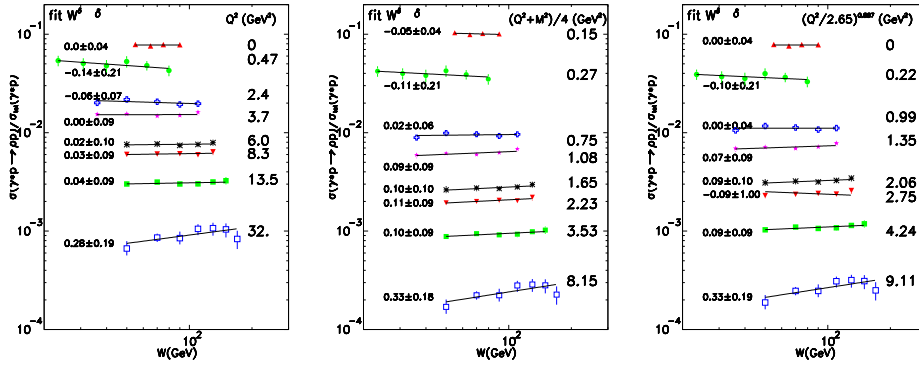


Fig. 11. The ratio of  $\sigma_{\rho^0}/\sigma_{tot}$  as a function of  $W$  for three choices of the effective scale;  $Q_{eff}^2 = Q^2$  (left),  $Q_{eff}^2 = (Q^2 + M^2)/4$  (middle) and  $Q_{eff}^2 = (Q^2/2.65)^{0.887}$  (right). The lines are fit of the form  $\sim W^\delta$  and the resulting values of  $\delta$  are given in the figures.

are used:  $Q_{eff}^2 = Q^2$ ,  $Q_{eff}^2 = (Q^2 + M^2)/4$ , and  $Q_{eff}^2 = (Q^2/2.65)^{0.887}$ . At each fixed scale, the  $W$  dependence is fitted to the form  $\sim W^\delta$  and the value of  $\delta$  is given in the figure. The ratio  $r_{\rho^0}$  seems to be constant with  $W$  and shows a possible  $W$  dependence only at the highest scale. We have shown earlier that this ratio is expected to grow with  $W$  like  $W^{2\lambda}$  in both the pQCD and the Regge approaches. This would thus indicate that the  $\lambda$  values obtained from this ratio are inconsistent with those obtained in the inclusive total deep inelastic cross section case.

We can in fact compare directly the values of  $\delta$  obtained from the  $W$  dependence of the  $\rho^0$  cross section, shown on the right-hand side of Fig. 4, to the  $\lambda$  values shown in Fig. 9, keeping in mind that  $\delta = 4\lambda$ . This is shown in Fig. 12, for the three effective scales mentioned above. For all three scales, the  $\lambda$  values obtained from the  $W$  dependence of the  $\rho^0$  are lower than those of the inclusive one for all but the highest effective scale of the  $\rho^0$ .

One way to find experimentally the right effective scale is to force the  $\lambda$  from the  $\rho^0$  to agree with that of the inclusive data. This is shown on

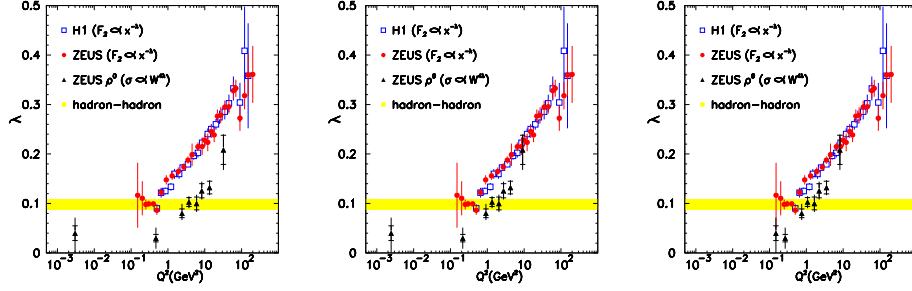


Fig. 12. Comparison of the  $\lambda$  values obtained from the exclusive electroproduction of  $\rho^0$  with those from the total inclusive cross section, as a function of  $Q^2$  for three choices of the effective scale of the  $\rho^0$ ;  $Q_{eff}^2 = Q^2$ (left),  $Q_{eff}^2 = (Q^2 + M^2)/4$  (middle) and  $Q_{eff}^2 = (Q^2/2.65)^{0.887}$  (right).

the left-hand side of Fig. 13. The resulting values of  $Q_{eff}^2$  are shown on

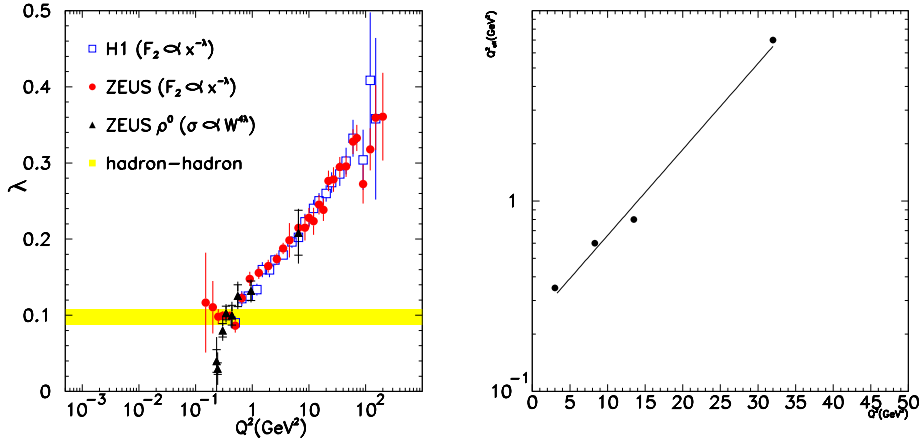


Fig. 13. (Left-hand side) The  $\lambda$  values obtained from the exclusive electroproduction of  $\rho^0$  together with those from the total inclusive cross section, as a function of  $Q^2$ . The effective scale of  $\rho^0$  was chosen so that the two  $\lambda$  agree. (Right-hand side) The effective scale of the  $\rho^0$ ,  $Q_{eff}^2$ , as a function of  $Q^2$ . The line is the result of an exponential fit to the data.

the right-hand side of Fig. 13. The effective scale is much smaller than  $(Q^2 + M_\rho)/4$  for low  $Q^2$  values. An exponential fit to the data, valid in the range where the measurements were done, results in the following ad hoc

parameterisation

$$Q_{eff}^2 = 0.23e^{0.1Q^2}. \quad (9)$$

The fact that the  $Q_{eff}^2$  in the exclusive  $\rho^0$  electroproduction is much smaller than  $Q^2$  of the photon might be due to the presence of the convolution of the soft  $\rho^0$  wave-function and the small size longitudinal photon wave-function. This is a clear sign of the interplay of soft and hard physics [4].

One can revisit now the  $r_{\rho^0}$  plot, using for the effective scale of the  $\rho^0$  as given in (9). This is shown in Fig. 14, where one can see now that the

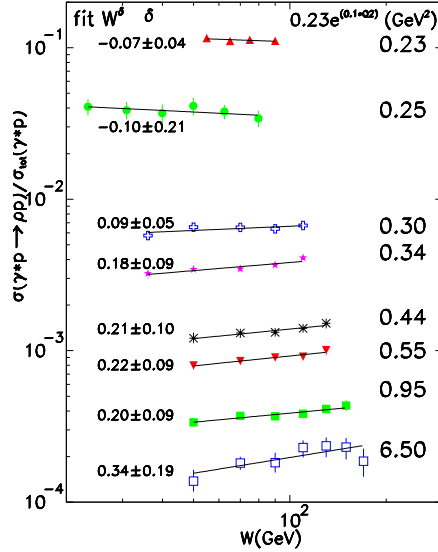


Fig. 14. The ratio of  $\sigma_{\rho^0}/\sigma_{tot}$  as a function of  $W$  for the effective scale  $Q_{eff}^2 = 0.23e^{0.1Q^2}$ . The lines are fit of the form  $\sim W^\delta$  and the resulting values of  $\delta$  are given in the figure.

ratio rises with  $W$ , as expected, even for the low effective scales.

Unfortunately, the precision of the data of exclusive electroproduction of  $J/\psi$  does not allow a similar study. The  $\lambda$  comparison for the  $J/\psi$  and inclusive data is shown in Fig. 15 for two effective scales,  $Q^2$  and  $(Q^2 + M^2)/4$ . Clearly  $Q_{eff}^2 = Q^2$  is inappropriate in the low  $Q^2$  region. However, the uncertainty of the data points of the exclusive channel does not allow further conclusions.

In principle, the question of the effective scale should not be an issue at all. If we were able to calculate QCD to all orders, we would know

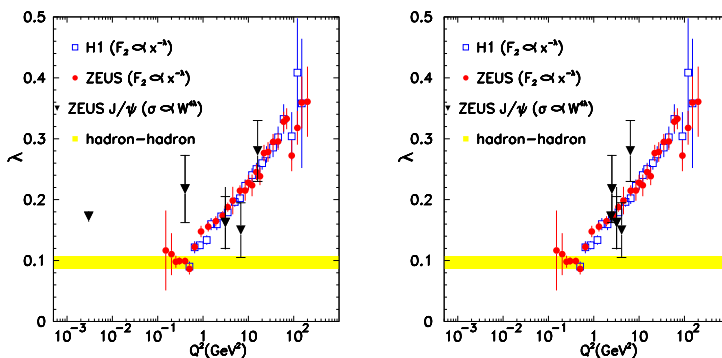


Fig. 15. Comparison of the  $\lambda$  values obtained from the exclusive electroproduction of  $J/\psi$  with those from the total inclusive cross section, as a function of  $Q^2$  for two choices of the effective scale of the interaction;  $Q_{eff}^2 = Q^2$  (left),  $Q_{eff}^2 = (Q^2 + M^2)/4$  (right).

exactly what is the right scale. However, as long as we do not yet have a full calculation, precision measurements of exclusive electroproduction of vector mesons would be helpful to resolve this problem.

## 5. $\lambda$ from inclusive diffraction

Following the comparison of  $\lambda$  from exclusive diffraction to that from total inclusive reactions in the previous section, it is of interest to make a similar comparison for inclusive diffraction. To this end, the recent data [18] on  $\alpha_P(0)$  as a function of  $Q^2$  is used, with the relation  $\lambda = \alpha_P(0) - 1$ . The results from the inclusive diffraction and the total inclusive reactions are shown in Fig. 16. The inclusive diffraction process shows a completely different behaviour from that of the total inclusive one; the values of  $\lambda$  seem to be  $Q^2$  independent and follow the expectations of a soft process. This indicates that the source of the large-rapidity-gap formation is a soft process.

One way to understand this feature is through the picture first advertised by Gribov [19] and by Feynman [20] who use the concept of 'wee' partons. The fact that one reaches high  $W$  values gives enough time for the cloud of partons to develop from 'perturbative partons' to 'non-perturbative partons', the latter being dressed large-size configurations, named as 'wee' partons. The large size configurations lead to a soft process in the formation of large rapidity gaps.

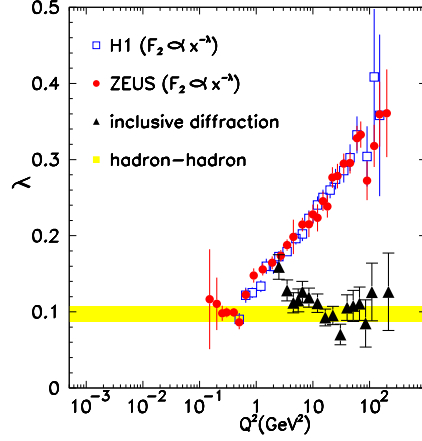


Fig. 16. Comparison of the  $\lambda$  values obtained from inclusive diffraction with those from the total inclusive cross section, as a function of  $Q^2$ .

## 6. Total photoproduction cross section at HERA

The first measurements [7, 21] of  $\sigma_{tot}(\gamma p)$ , though having large uncertainties, were enough to establish that the photon behaves at large energies as a hadron. Later attempts to improve the precision of the measurement [22, 23] showed that while the statistical uncertainty can be much reduced, the systematic uncertainty is still large (see Fig. 17) and can not allow a precise determination of the energy dependence.

During the last period of HERA running, the proton energy was changed from 920 GeV (high energy run - HER) to 575 GeV (medium energy run - MER) and to 460 GeV (low energy run - LER). The main purpose was to measure the longitudinal structure function  $F_L$  of the proton. In addition, a special photoproduction trigger was implemented to extract the value of  $\lambda$  by measuring ratios of cross sections at different  $W$  values and thus minimizing the systematic uncertainties.

Assuming  $\sigma \sim W^\delta$  [22],

$$r = \frac{\sigma(W_1)}{\sigma(W_2)} = \left( \frac{W_1}{W_2} \right)^\delta. \quad (10)$$

Experimentally,

$$\sigma = \frac{N}{A \cdot \mathcal{L}}, \quad (11)$$

where  $A$ ,  $\mathcal{L}$  and  $N$  are the acceptance, luminosity and number of measured

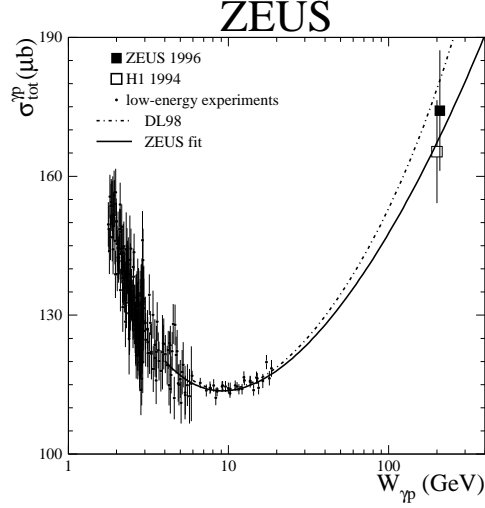


Fig. 17. The photon-proton total cross section as a function of the photon-proton center-of-mass energy.

events, respectively, and therefore

$$r = \frac{N_1}{N_2} \cdot \frac{A_2}{A_1} \cdot \frac{\mathcal{L}_2}{\mathcal{L}_1}, \quad (12)$$

where the index 1(2) denotes measurements performed at  $W_1$  ( $W_2$ ). The acceptance for  $\gamma p$  events at HERA depends mainly on the detector infrastructure in the electron (rear) direction. If the change in the  $W$  value results from changing the proton energy, the acceptance is likely to remain the same independent of  $W$  and the ratio of acceptances will drop out in Eq. (12).

A preliminary measurement, using HER and LER data, was presented at DIS08 [24]. The value of  $\delta$  as obtained from  $r$  was

$$\delta = 0.140 \pm 0.014(\text{stat.}) \pm 0.042(\text{syst.}) \pm 0.100(6\text{mT}), \quad (13)$$

which translates into

$$\lambda = 0.070 \pm 0.007(\text{stat.}) \pm 0.021(\text{syst.}) \pm 0.050(6\text{mT}). \quad (14)$$

This result is consistent with earlier determinations of  $\lambda$  (also denoted as  $\epsilon$ ), however has the advantage of being obtained from a single experiment and being model independent.

The statistical uncertainty will be improved in the future by including the data taken with a third proton beam energy (MER). The systematic uncertainty will improve by a better understanding and calibration of the tagger of the scattered electron (6mT).

## 7. Summary

The HERA data are a good source to observe the interplay of soft and hard dynamics, through the study of energy dependences of different processes.

The process of exclusive electroproduction of vector mesons at high scales is a good source to study perturbative QCD. It is important to understand the issue of the effective scale. For the  $\rho^0$ , the effective scale is much smaller than the  $Q^2$  of the photon. Better precision measurements are needed for the  $\phi$ ,  $J/\psi$  and DVCS to get a determination of the effective scale in these processes.

There are plans to measure precisely the energy dependence of the  $\gamma p$  total cross section. This would set the baseline of soft interactions to which  $\gamma^* p$  results can be compared.

## 8. Acknowledgments

It is a pleasure to thank the organisers for an excellent and pleasant meeting organised in memory of Prof. Jan Kwiecinski.

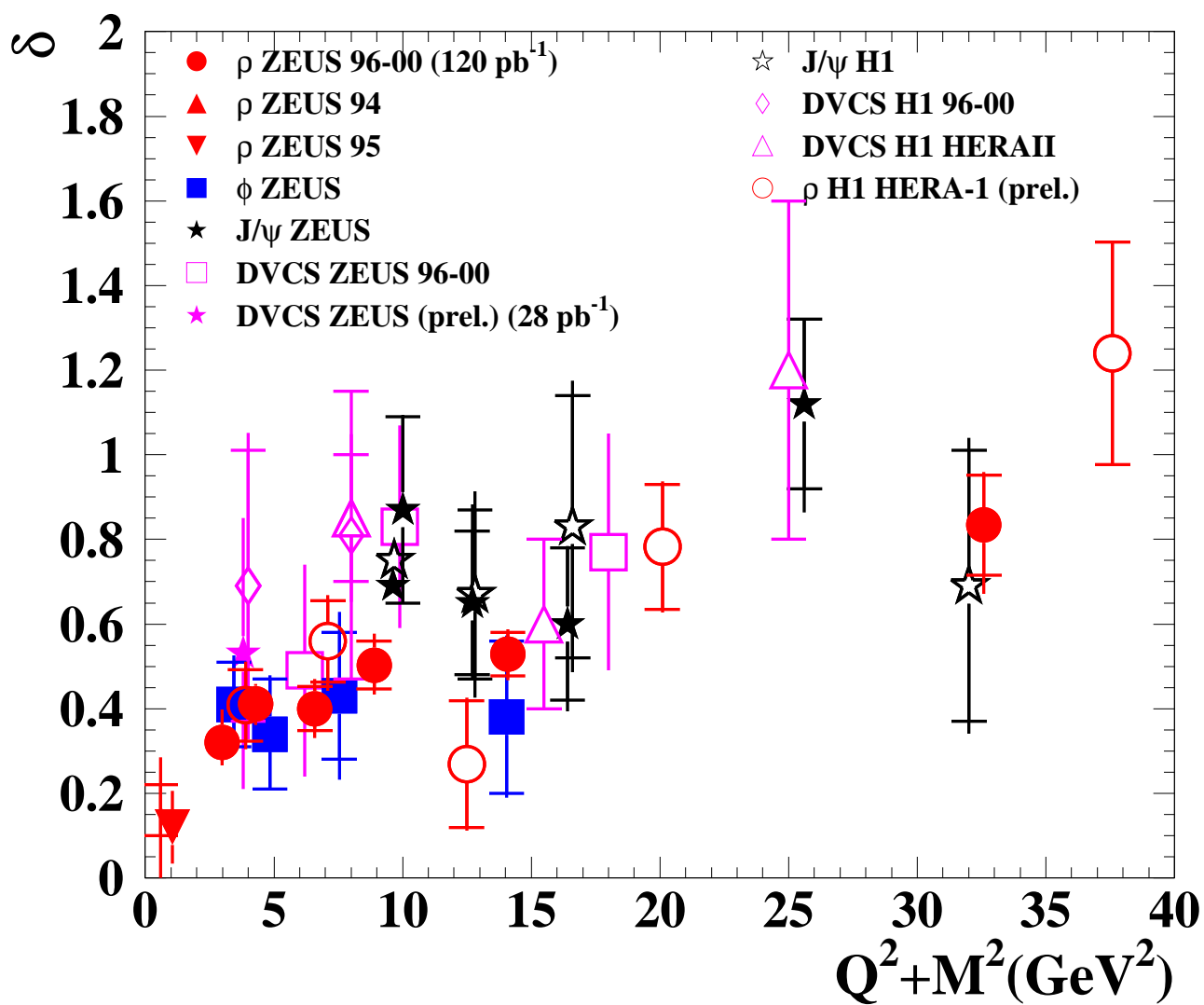
This work was supported in part by the Israel Science Foundation (ISF).

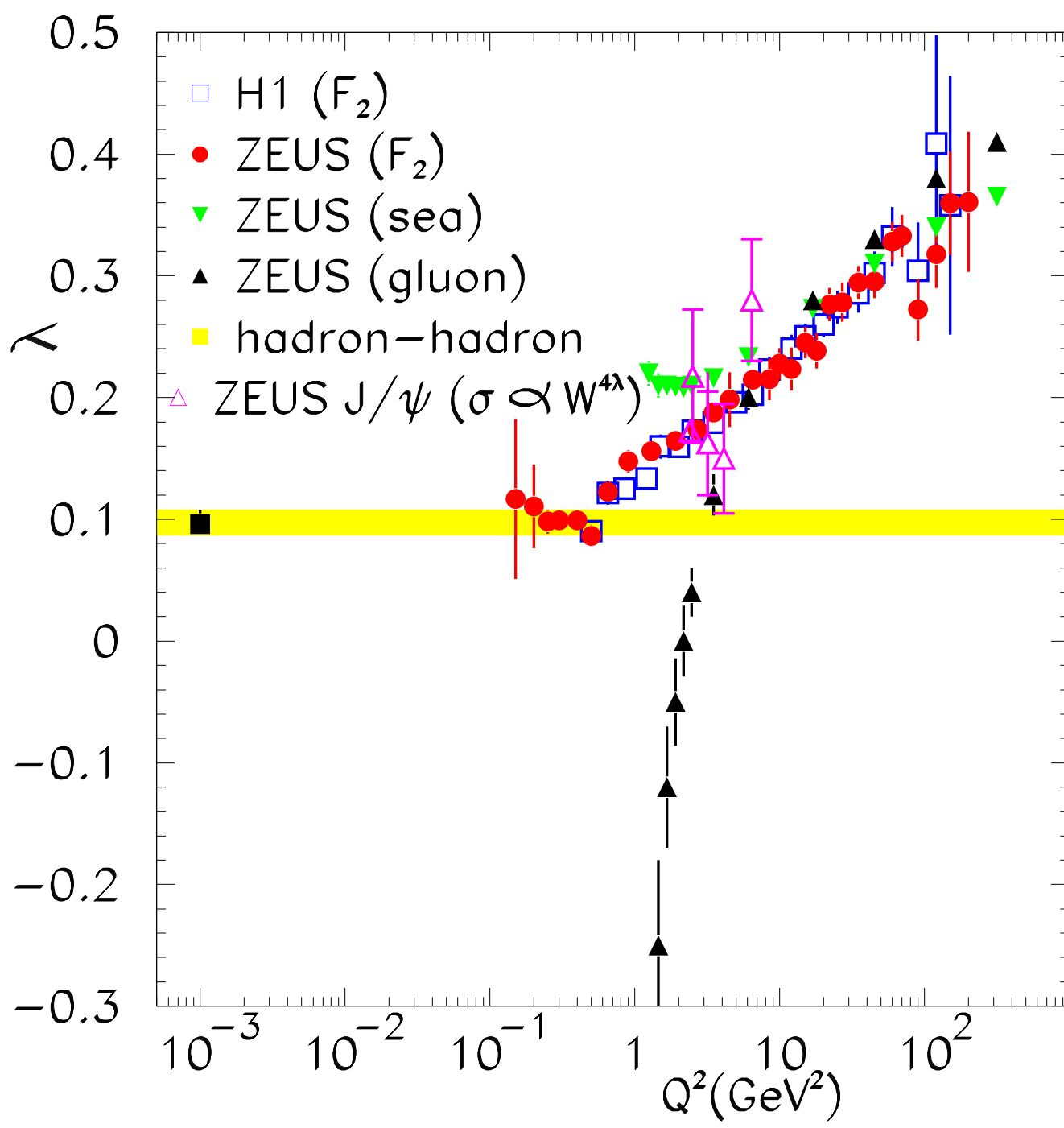
## REFERENCES

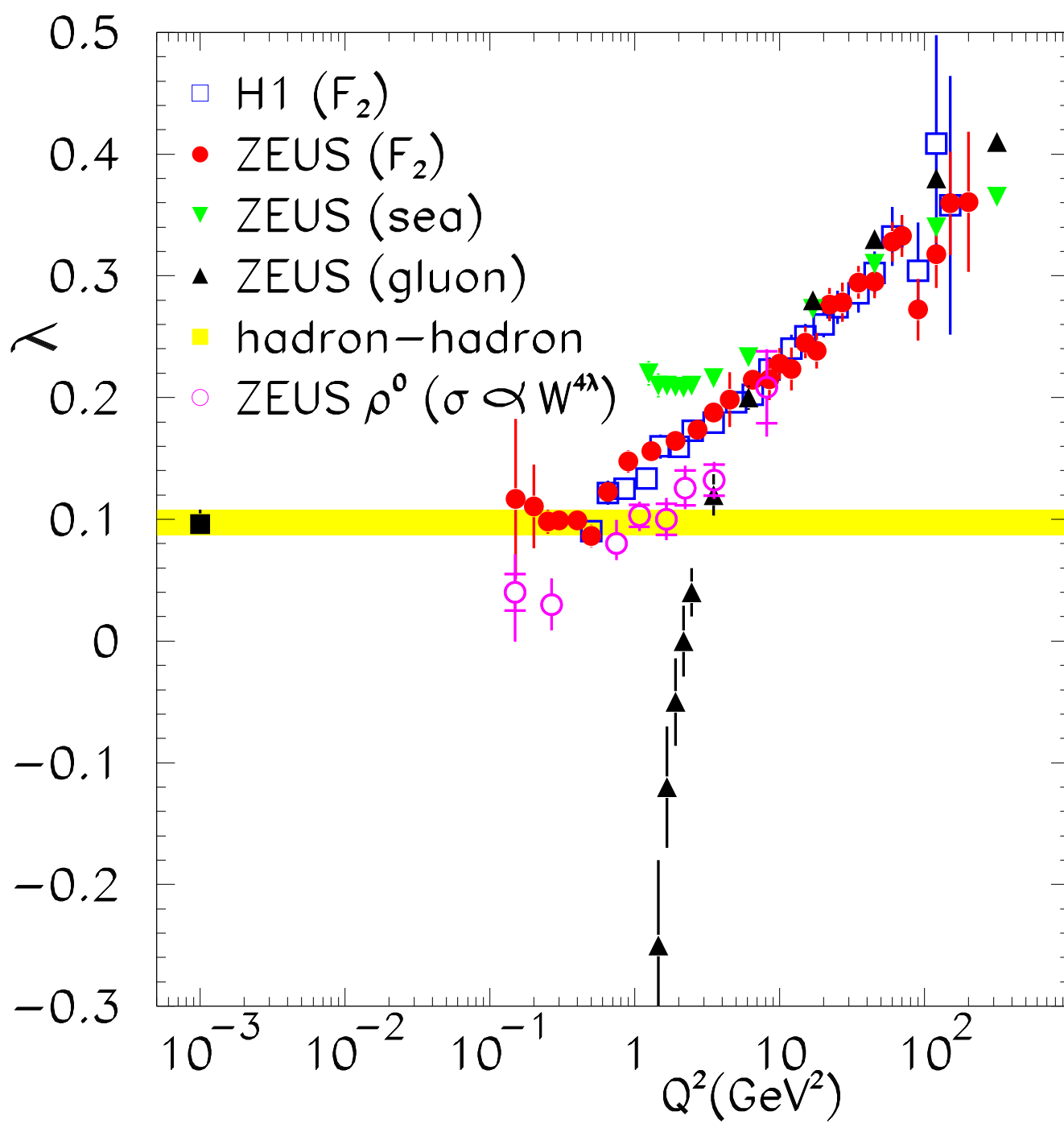
- [1] A. Donnachie and P.V. Landshoff, *Total cross sections*, Phys. Lett. **B 296**, 227 (1992).
- [2] ZEUS Collab., S. Chekanov et al., *Exclusive electroproduction of  $J/\psi$  mesons at HERA*. Nucl. Phys. **B 695**, 3 (2004).
- [3] H1 Collab., A. Aktas et al., *Elastic  $J/\psi$  production at HERA.*, Eur. Phys. J. **C 46**, 585 (2006).
- [4] H. Abramowicz, L. Frankfurt and M. Strikman, *Interplay of hard and soft physics in small  $x$  deep inelastic scattering.*, Survey High Energy Phys. **11**, 51 (1997).
- [5] P.D.B. Collins, *An introduction to Regge theory and high energy physics.*, Cambridge University Press, 1977.
- [6] J.R. Cudell et al., *High-energy forward scattering and the Pomeron: Simple pole versus unitarized models*, Phys. Lett. **B 395**, 311 (1997).
- [7] ZEUS Collab., M. Derrick et al., *A measurement of  $\sigma_{tot}(\gamma p)$  at  $\sqrt{s}=210$  GeV*, Phys. Lett. **B 293**, 465 (1992).
- [8] S.J. Brodsky et al., *Diffraction leptoproduction of vector mesons in QCD.*, Phys. Rev. **D 50**, 3134 (1994).
- [9] ZEUS Collab., S. Chekanov et al., *Exclusive  $\rho^0$  production in deep inelastic scattering at HERA.*, PMC Phys. **A 1**, 6 (2007).

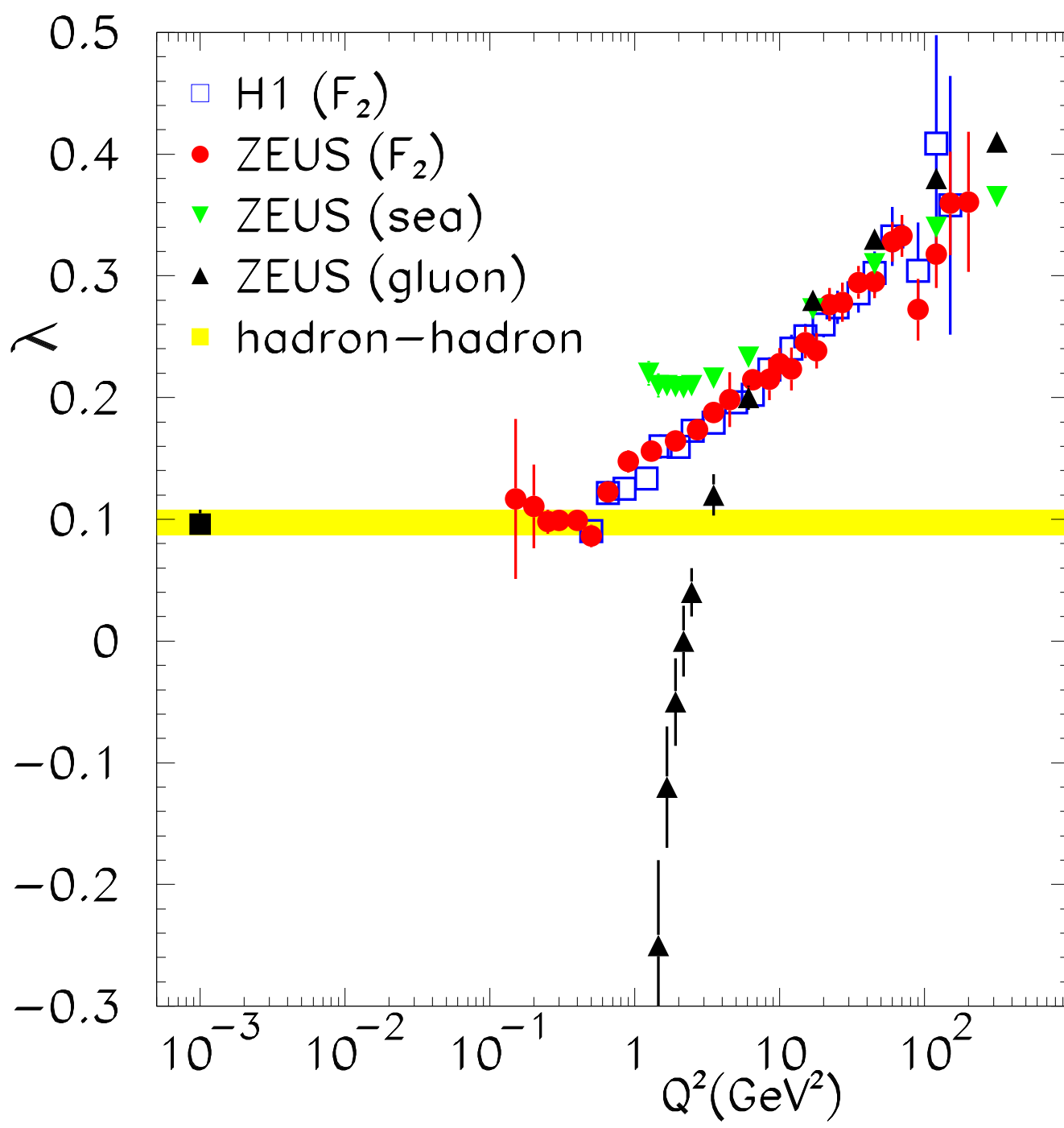


- [10] H1 Collab., C. Adloff et al., *Elastic electroproduction of  $\rho$  mesons at HERA.*, Eur. Phys. J. **C 13**, 371 (2000).
- [11] ZEUS Collab., S. Chekanov et al., *Exclusive electroproduction of  $\phi$  mesons at HERA.*, Nucl. Phys. **B 718**, 3 (2005).
- [12] H1 Collab., C. Adloff et al., *Measurement of elastic electroproduction of  $\phi$  mesons at HERA.*, Phys. Lett. **B 483**, 360 (2000).
- [13] ZEUS Collab., S. Chekanov et al., *A measurement of the  $Q^2$ ,  $W$  and  $t$  dependences of deeply virtual Compton scattering at HERA.*, accepted to JHEP (2009), arXiv:0812.2517 [hep-ex].
- [14] H1 Collab., A. Aktas et al., *Measurement of Deeply Virtual Compton Scattering and its  $t$ -dependence at HERA.*, Phys. Lett. **B 659**, 796 (2008).
- [15] M.G. Ryskin, *Diffraction  $J/\psi$  electroproduction in LLA QCD.*, Z.Phys. **C 57**, 89 (1993).
- [16] L. Frankfurt, W. Koepf and M. Strikman, *Diffraction heavy quarkonium photoproduction and electroproduction in QCD.*, Phys. Rev. **D 57**, 512 (1998).
- [17] M. Strikman, private communication.
- [18] ZEUS Coll., *Deep inelastic scattering with leading protons or large rapidity gaps at HERA.*, S. Chekanov et al., Nucl. Phys. **B 816**, 1 (2009).
- [19] V.N. Gribov, *Material of the 8th winter school of the Leningrad Institute of Nuclear Physics (in Russian).*, 1973. (Preprint hep-ph/0006158 (English translation), 2000.)
- [20] R.P. Feynman, *Photon-hadron interactions.*, (Benjamin, Reading, Massachusetts, 1972).
- [21] H1 Collab., T. Ahmed et al., *Total photoproduction cross section measurement at HERA energies*, Phys. Lett. **B 299**, 374 (1993).
- [22] ZEUS Collab., S. Chekanov et al., *Measurement of the photon-proton total cross section at a center-of-mass energy of 209 GeV at HERA.*, Nucl. Phys. **B 627**, 3 (2002).
- [23] H1 Collab., S. Aid et al., *Measurement of the total photon-proton cross-section and its decomposition at 200 GeV center-of-mass energy.*, Z. Phys. **C 69**, 27 (1995).
- [24] A. Levy, *Energy dependence of  $\sigma_{tot}(\gamma p)$  at HERA*, Published in \*London 2008, Deep inelastic scattering\* 48, arXiv:0807.0191 [hep-ex].

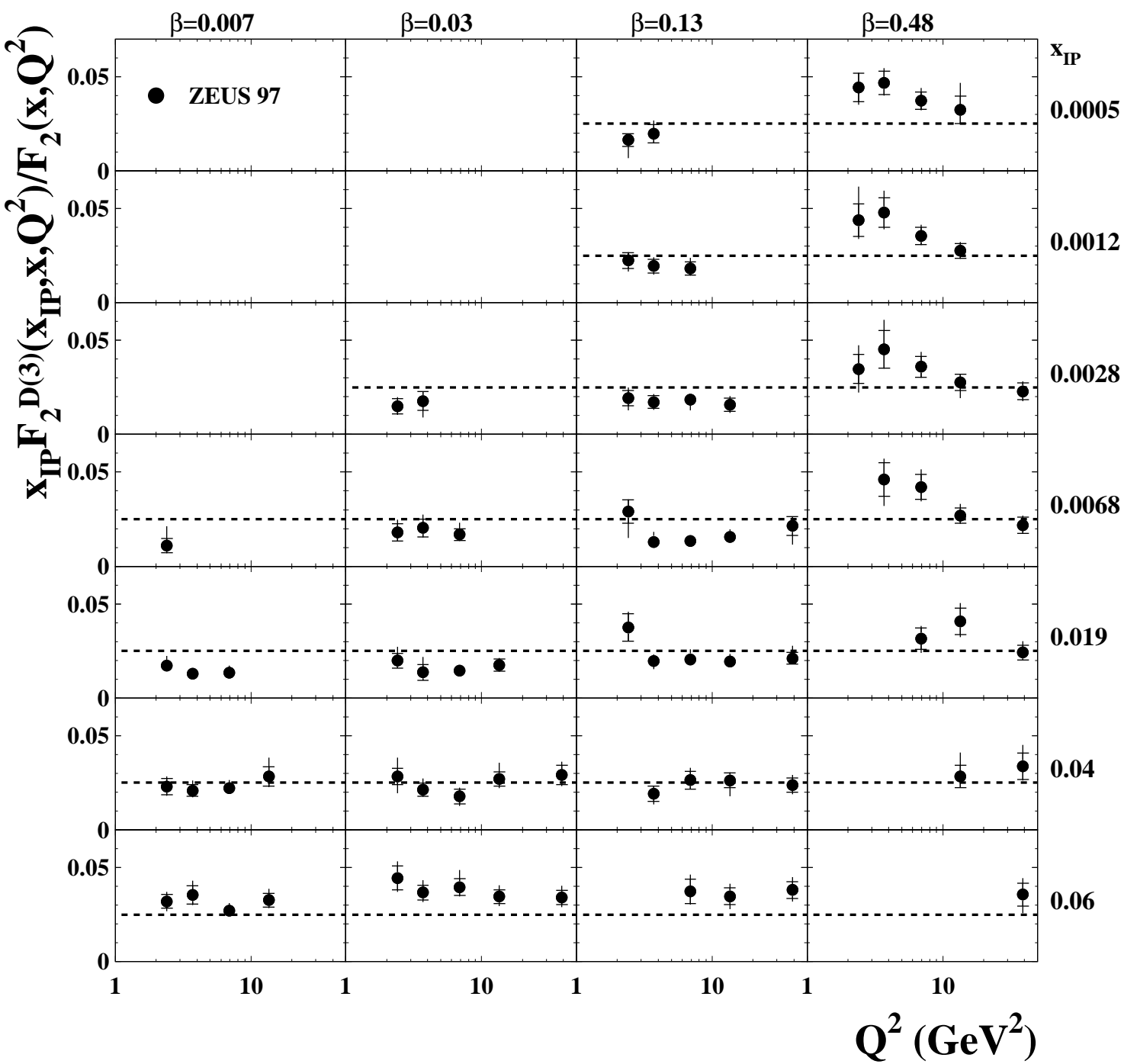


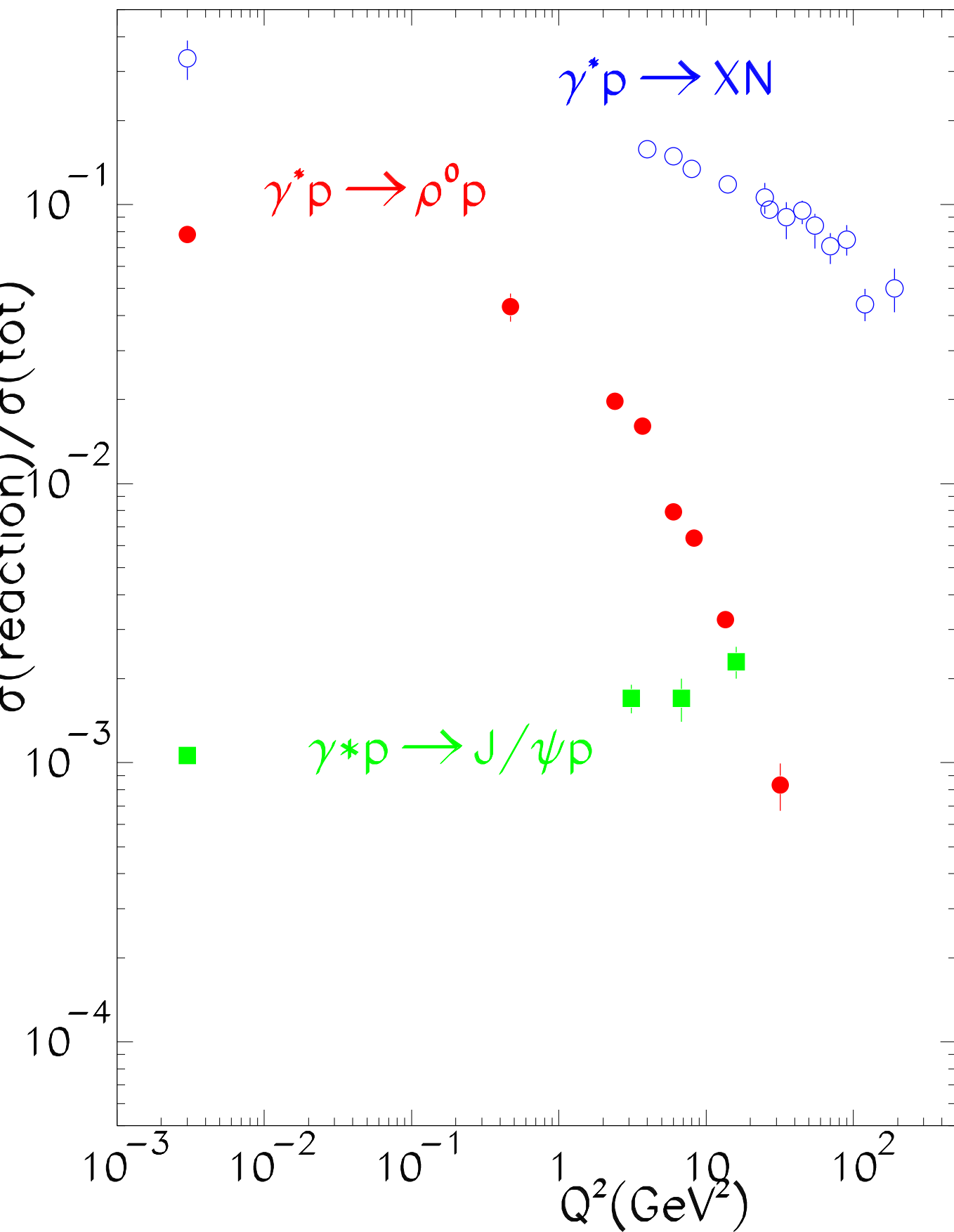






# ZEUS





cross section ( $\mu\text{b}$ )

